RAPID COMMUNICATIONS

PHYSICAL REVIEW B VOLUME 43, NUMBER 8 15 MARCH 1991-I

Polarized-cathodoluminescence study of uniaxial and biaxial stress in GaAs/Si

D. H. Rich, A. Ksendzov, R. W. Terhune, F. J. Grunthaner, and B. A. Wilson
Center for Space Microelectronics Technology, Jet Propulsion Laboratory, California Institute of Technology, 4800 Oak Grove Drive, Pasadena, California 91109

H. Shen* and M. Dutta
U.S. Army Electronics Technology and Devices Laboratory, Fort Monmouth, New Jersey 07703

S. M. Vernon and T. M. Dixon
Spire Corporation, Bedford, Massachusetts 01730
(Received 30 November 1990)

The strain-induced splitting of the heavy-hole (hh) and light-hole (lh) valence bands for 4-μm-thick GaAs/Si is examined on a microscopic scale using linear polarized-cathodoluminescence imaging and spectroscopy. The energies and intensities of the hh- and lh-exciton luminescence are quantitatively analyzed to determine spatial variations in the stress tensor. The results indicate that regions near and far from the microcracks are primarily subject to uniaxial and biaxial tensile stresses, respectively. The transition region where biaxial stress gradually converts to uniaxial stress is analyzed, and reveals a mixing of lh and hh characters in the strain-split bands.

In the past decade, improvements in epitaxial-growth techniques have made feasible the hybridization of GaAs and Si technologies for applications of high-speed electronic and optoelectronic devices, despite the 4.1% lattice mismatch. The ratio of the GaAs and Si thermal-expansion coefficients is about 2.5 at typical growth temperatures in excess of 700 °C, and the subsequent cooling to room temperatures results in a large tetragonal distortion which can cause wafer bowing and the formation of microcracks to relieve partially the thermal stress. The effects of stress on the splitting of the $j=\frac{3}{2}$ heavy-hole (hh; $m_j=\pm\frac{3}{2}$) and light-hole (lh; $m_j=\pm\frac{1}{2}$) bands at $\mathbf{k}=\mathbf{0}$ have been previously studied by several authors using photoluminescence (PL),[1-8] photoluminescence excitation (PLE),[1,2,9] cathodoluminescence (CL),[10] and photoreflectance (PR);[11,12] optical transitions involving these states exhibit polarization selection rules which depend on the strain.[4,12-14]

In this paper, we present the results of a novel approach in which linearly polarized CL scanning electron microscopy (SEM) is used to analyze spatial variations in the stress tensor for GaAs/Si. Yacobi and co-workers,[10] using CL, have demonstrated the presence of local variations in the luminescence near microcracks caused by variations in stress. With the enhancement of a linear-polarization-detection scheme, we demonstrate that a quantification of the exciton luminescence intensities and energies in the CL spectra can be performed; this leads to a definitive evaluation of the micrometer-scale spatial variations of the hh and lh characters in the strain-split valence bands. The present approach, in conjunction with polarization selection rules which depend on the form of the stress tensor, enables a determination of the spatial distribution of the stress. Scanning monochromatic CL images are presented and reveal a polarization anisotropy within the sample. From the results, we show that the stress is predominantly uniaxial along the microcracks and predominantly biaxial in the regions between the cracks.

The samples examined in this study were grown by atmospheric-pressure metal-organic chemical-vapor deposition (MOCVD) at the Spire Corporation.[15] A three-step method was used to grow the sample and is described here: the Si substrate [oriented 2° off (001) in the ⟨110⟩ direction] was heated in hydrogen to over 1000 °C to desorb the oxide layer, the temperature was then lowered to about 400 °C for the nucleation and growth of 200 Å of GaAs, and finally, a thick GaAs layer was deposited at typical MOCVD conditions using a 700 °C growth temperature to give a 4-μm thickness.

Cathodoluminescence measurements were performed with a JEOL 840-F field-emission SEM. The CL optical-collection system and cryogenic-specimen stage were designed and constructed at the Jet Propulsion Laboratory. The luminescence emitted from the sample was collected with an ellipsoidal mirror which focuses the radiation onto a coherent optical-fiber bundle leading outside the SEM vacuum chamber to a 0.25-m-focal-length monochromator. The coherency of the bundle allows for a direct imaging of light at the second ellipsoidal focus into the entrance slit of the monochromator. The bundle acts as an efficient polarization scrambler, and to perform polarization measurements a rotatable vacuum polarizer was mounted directly in front of the bundle. In order to account for polarization-mixing effects caused by reflection at the mirror, e.g., due to finite solid angle of collection and changes in the electric field's (E) phase and amplitude, a linearly polarized Lambertian (cosine) source was placed at the focus to simulate emission from the sample. The intensity-extinction ratio $I_\perp/I_\parallel$, measured by rotating one polarizer 90° with respect to the other, departed from the ideal value of 0 and was found to be $I_\perp/I_\parallel\sim 0.27$. The slit width of the monochromator was chosen to give a spectral resolution of 1 nm. An electron-beam current of 100 pA at an accelerating voltage of 40 kV (giving a spatial resolution of 2 to 3 μm) was used to probe the GaAs/Si sample which was maintained at a temperature

 ©1991 The American Physical Society

of about 77 K.

Scanning monochromatic images of GaAs/Si at $h\nu = 1.494$ eV are shown in Fig. 1, where regions of increasing luminescence signal are represented by areas of lighter shades. Figure 1(a) shows an image taken without a polarizer, and reveals bands of bright luminescence oriented along both $\langle 110 \rangle$ and $\langle 1\bar{1}0 \rangle$ directions. The dark narrow lines located in each band indicate the positions of the microcracks, and the luminescence intensity is seen to diminish at the cracks. By surveying the entire sample, the cracks were found to occur predominantly along $\langle 110 \rangle$, and $\langle 1\bar{1}0 \rangle$-oriented cracks were mainly found to serve as beginning and ending points for the $\langle 110 \rangle$-oriented cracks. In Fig. 1, random fluctuations in the local CL intensity are observed in the regions between the microcracks. This is attributed to the presence of a large number of defects (e.g., stacking faults and dislocations), which were also observed by Yacobi and co-workers.[10] In Figs. 1(b) and 1(c), the images were taken with the linear polarizer oriented so that emission with electric field parallel and perpendicular to $\langle 110 \rangle$, respectively, could be detected. It is apparent that for the case $\mathbf{E} \perp \langle 110 \rangle$ ($\mathbf{E} \perp \langle 1\bar{1}0 \rangle$) there is a significant increase in brightness near the $\langle 110 \rangle$-($\langle 1\bar{1}0 \rangle$-) oriented cracks relative to the case $\mathbf{E} \parallel \langle 110 \rangle$ ($\mathbf{E} \parallel \langle 1\bar{1}0 \rangle$), which indicates a polarization anisotropy for the emission from the vicinity of the cracks. The intensity of emission from regions away from the cracks was observed to be independent of the polarization angle.

These results were further investigated by localized CL spectroscopy. Particular cracks shown in Fig. 1(a) running along $\langle 1\bar{1}0 \rangle$ and $\langle 110 \rangle$ are labeled as C_A and C_B, respectively. The dashed lines in Fig. 1(a) indicate paths where the electron beam was positioned relative to the cracks. Localized spectra (dots) taken from regions near C_B are shown in Fig. 2, and for each spectrum the perpendicular distance from the center of the crack (ΔX) is indicated. Two spectra, with the polarizer set to detect emission for $\mathbf{E} \perp C_B$ and $\mathbf{E} \parallel C_B$, respectively, are shown for each distance ΔX. The displayed spectra have been renormalized to have equal peak heights, and the multiplication factors used to scale the $\mathbf{E} \parallel C_B$ spectrum relative to $\mathbf{E} \perp C_B$ in each pair are indicated. For electron-beam positions

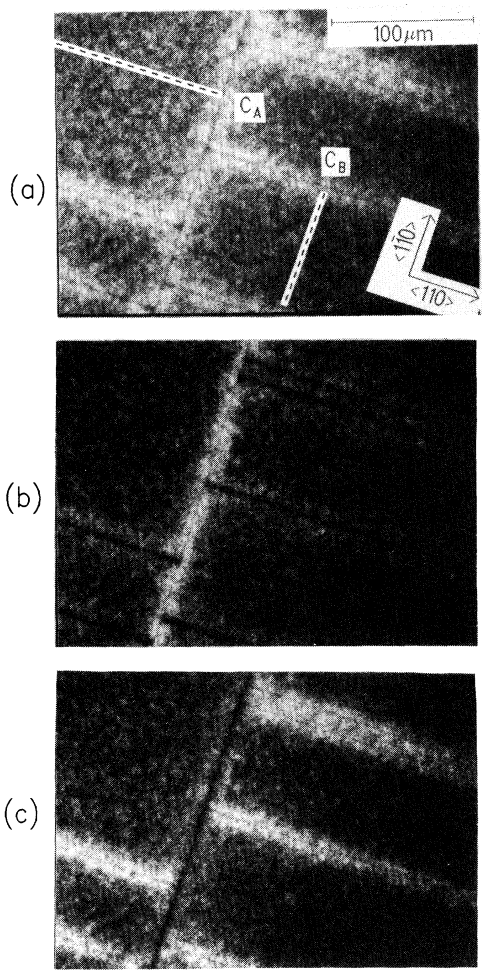

FIG. 1. Scanning monochromatic CL images at $h\nu = 1.494$ eV for the GaAs/Si sample with (a) no polarizer, (b) emission with $\mathbf{E} \parallel \langle 110 \rangle$, (c) and $\mathbf{E} \perp \langle 110 \rangle$. Two microcracks which run perpendicular and parallel to $\langle 110 \rangle$ are labeled C_A and C_B, respectively. The dashed lines indicate the positions of the electron beam during the localized spectroscopy measurements.

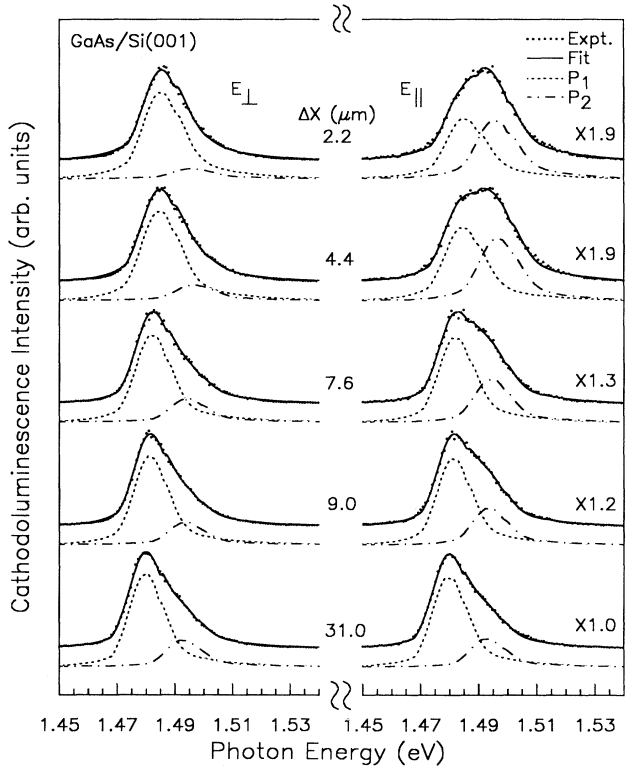

FIG. 2. Linear polarized localized cathodoluminescence spectra near the region of the C_B microcrack of Fig. 1. Two spectra (dots), obtained with polarization conditions $\mathbf{E} \perp C_B$ and $\mathbf{E} \parallel C_B$ (labeled $\mathbf{E}_\perp$ and $\mathbf{E}_\parallel$, respectively, in the figure), are shown for each distances (ΔX) from the crack. The results of the fits to the spectra (solid lines) and the individual strain-split P_1 (dashed lines) and P_2 (dash-dotted lines) components are shown. The spectra for $\mathbf{E} \parallel C_B$ were scaled up relative to the $\mathbf{E} \perp C_B$ spectra by the factors indicated.

approaching the crack, the intensities of $\mathbf{E}\|C_B$ spectra are seen to decrease relative to the $\mathbf{E}\perp C_B$ spectra. Also, the center of gravity for the $\mathbf{E}\|C_B$ spectra is seen to shift toward higher energy relative to its $\mathbf{E}\perp C_B$ counterpart. In the simplest model, the orientation of the polarizer can affect only the intensity of the luminescence originating from a particular transition, and not the energy of the transition. Therefore, the spectra are composed of more than one transition with different polarization selection rules.

In order to quantify these results, we have decomposed the CL line shapes into strain-split components P_1 and P_2 for various spectra taken along the dashed lines shown in Fig. 1 (including all spectra shown in Fig. 2). We employ a model that uses functions $F_i(E)$ and $G_i(E)$ to represent each luminescence component:

$$F_i(E)=\begin{cases}\exp\left[-\left(\dfrac{E-E_{gi}+E_x}{\beta}\right)^2\right], & E\geq E_{0i}\,,\\ \exp\left[\dfrac{E-E_{0i}}{\alpha}-\left(\dfrac{E_{0i}-E_{gi}+E_x}{\beta}\right)^2\right], & E<E_{0i}\,,\end{cases} \tag{1}$$

and

$$G_i(E)=\begin{cases}(\sqrt{E/E_{gi}-1})\exp\left[-\dfrac{E-E_{gi}}{kT}\right], & E\geq E_{gi}\,,\\ 0, & E<E_{gi}\,,\end{cases} \tag{2}$$

where i is an index referring to the strain split bands ($i=1,2$), E_{gi} is the band gap for each of the strain-split bands, and E_x is the exciton binding energy which is 5 meV in GaAs. Due to random fluctuations in strain and a large density of defects, we expect the dominant broadening mechanism to be inhomogeneous, and $F_i(E)$ represents the exciton luminescence which contains a Gaussian term centered at the exciton energy $(E_{gi}-E_x)$ with a Gaussian width β. For luminescence in GaAs, the low-energy tail is known to decay exponentially with energy,[16] and the parameter E_{0i} represents the transition energy at which Gaussian behavior becomes exponential with decay constant α. $G_i(E)$ represents the higher-energy band-to-band transitions,[3] and this can dominate the luminescence when $kT\gg E_x$, where T is the carrier temperature, and k is the Boltzmann constant. The total CL line shape is obtained by summing the individual contributions from both components and is given by

$$L_{\|,\perp}(E)=\sum_{i=1,2}S_i[F_i(E)+RG_i(E)]\,, \tag{3}$$

where S_i is the intensity of the P_i component, and R represents the intensity of the band-to-band transitions relative to the exciton transition. Spectra for both $E_\|$ and $E_\perp$ polarizations for a given point relative to the crack are simultaneously fit so as to minimize a composite χ^2 statistic. The energy positions E_{gi} and line-shape parameters E_{0i}, β, α, T, and R are constrained to be invariant for each pair of $E_\|$- and $E_\perp$-polarized spectra because, according to the model, only the intensity S_i of each transition can vary with polarization direction, not the energy position or line shape. With this constraint, the calculated value of the polarization anisotropy for the P_i component of the spectrum is equal simply to $S_{i\perp}/S_{i\|}$.

The fits were performed for 14 pairs of C_A- and 18 pairs of C_B-type spectra. The results of the fits (solid lines) are shown in Fig. 2, and the individual components P_1 and P_2 are shown offset below the spectra. The large polarization anisotropy in the P_1 and P_2 behaviors is apparent. The measured integrated intensity ratios for each pair of spectra $I_\perp/I_\|$ and the ratios $S_{i\perp}/S_{i\|}$ from the fits are shown in Fig. 3 as a function of the distance ΔX from the center of the cracks. The behaviors of P_1 and P_2 near both cracks C_A and C_B are identical within the experimental error. Despite the large difference in abundance between the two types of cracks, the stress-reduction mechanisms are very similar. The average values and uncertainties obtained for $(E_{gi}-E_{0i})$, β, α, T, and R are 16.2 ± 1.1, 8.2 ± 0.4, 7.2 ± 1.1 meV, 123 ± 6 K, and 3.82 ± 0.54, respectively.

It is our hypothesis that the large polarization anisotropy of hh and lh exciton transitions associated with uniaxial tensile stress near the cracks is responsible for this intensity and line-shape behavior. In the regions far from the cracks, the GaAs is widely believed to be under biaxial tensile stress, which results in a stress tensor (σ) with equal components $\sigma_\|=\sigma_\perp\neq0$. Near the cracks, the GaAs is free to relax, which results in a uniaxial stress with $\sigma_\perp=0$. The effects of uniaxial and biaxial stress on the hh and lh wave functions in GaAs have been previously calcu-

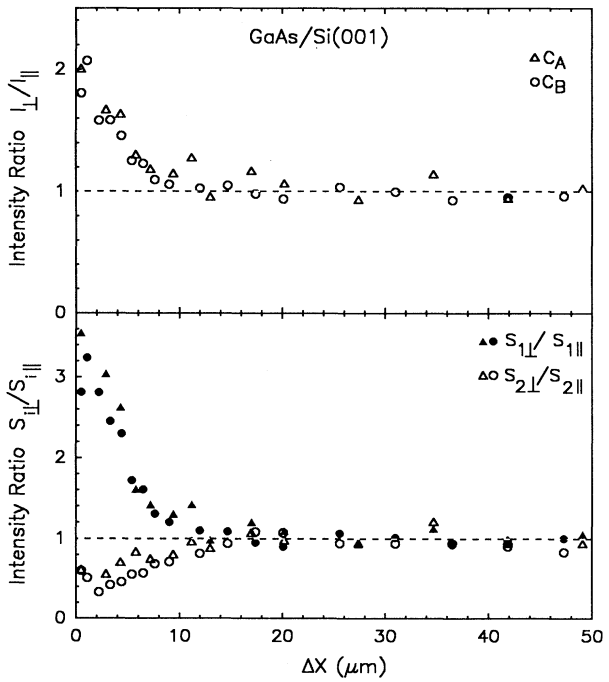

FIG. 3. Polarized intensity ratios obtained from the local spectroscopy measurements. In the upper portion of the figure, the total integrated intensity ratios $I_\perp/I_\|$ of the spectra as a function of the perpendicular distance from the C_A (triangles) and C_B (circles) microcracks are shown. In the lower portion of the figure, the intensity ratios $S_{1\perp}/S_{1\|}$ (filled symbols) and $S_{2\perp}/S_{2\|}$ (open symbols) of the individual strain-split components P_1 and P_2 are shown; the triangles and circles indicate the results for C_A and C_B cracks, respectively.

lated.[13,14] For the case of biaxial tensile stress here, the preferential direction for the quantization of the hole angular momentum (m_j) is along ⟨001⟩, emission along this direction is unpolarized in the (001)-surface plane, and the lh exciton is the lowest-energy transition. Thus, the observation of no polarization dependence, as shown in Fig. 3, for regions more than ~ 15 μm away from the microcracks is consistent with the selection rules for biaxial stress. We attribute the P_1 and P_2 components of the fits in this region to lh and hh transitions, respectively. From the fits of all spectra for $\Delta X \gtrsim 15$ μm, the average values obtained for S_2/S_1 and $E_{g2}-E_{g1}$ are 0.30 ± 0.02 and 12.9 ± 0.7 meV, respectively, and this yields a hh-to-lh oscillator-strength ratio of 2.3 ± 0.4 in reasonable agreement with the theoretical value of 3.[4,12] For biaxial tensile stress in GaAs/Si(100), the lh to hh energy splitting is known to increase at a rate of ~ 6.2 meV/kbar.[6,13,14] A 12.9-meV splitting for $\Delta X \gtrsim 15$ μm is thus indicative of a 2.1 ± 0.1 kbar stress, which is in good agreement with linear polarized PR and PL,[4,12] and PLE results.[2]

For pure uniaxial tensile stress along ⟨110⟩ (⟨1$\bar{1}$0⟩), the preferential direction for m_j is along ⟨110⟩ (⟨1$\bar{1}$0⟩), and the hh exciton is the lowest energy transition.[13] Regions of pure biaxial and pure uniaxial stress must have a reversed energy order for the hh and lh exciton transitions; a quantification of the polarization dependence of the exciton luminescence is needed to confirm this energy reversal. The hh exciton emission along ⟨001⟩ is totally linearly polarized perpendicular to the crack, while the lh exciton is partially polarized. The minimum value obtained for $S_{1\parallel}/s_{1\perp}$ is ~ 0.28 at $\Delta X = 0.5$ μm (from Fig. 3), and this is close to the result obtained by using a linearly polarized source for calibration, as described earlier. Thus, the large polarization anisotropy shown in Fig. 3 for small ΔX is due to the uniaxial character of the stress, and the P_1 and P_2 components of the fits are identified with the hh and lh transitions, respectively, for regions $\Delta X \lesssim 2$ μm. For $\Delta X \lesssim 15$ μm the values for $S_{2\perp}/S_{2\parallel}$ are seen to decrease below 1, and this is consistent with the polarization dependence of the lh wave function for uniaxial stress which, ideally, should yield $S_{2\perp}/S_{2\parallel} = 0.25$. Also, there is an apparent mixing of lh and hh states for $2 \lesssim \Delta X \lesssim 15$ μm, as evidenced by the intensity behaviors of the P_1 and P_2 components in Fig. 3, and this indicates the gradual reduction of $\sigma_\perp$ in this range.[17] If we assume that no relaxation of $\sigma_\parallel$ occurs, the value of $E_{g1}-E_{g2}$ at $\Delta X \approx 0$ can be compared with predicted values using the 2.1 ± 0.1-kbar stress found in the biaxial region. Pollack and Cardona have shown that for a ⟨110⟩ uniaxial stress in GaAs, the hh-to-lh energy splitting increases at a rate of ~ 5.6 meV/kbar,[13] and, consequently, a splitting of 11.7 meV is predicted. This is in good agreement with the value of 10.9 ± 0.5 meV obtained from the fits for $\Delta X \lesssim 2$ μm, and this decrease in the hh-to-lh energy splitting relative to that obtained for the biaxially stressed region is consistent with a 1–2 meV decrease previously observed in PR and PLE measurements.[2,12]

In conclusion, the polarization anisotropy of the luminescence emitted from regions near microcracks in GaAs/Si has been demonstrated using high-resolution CL imaging and spectroscopy. By utilizing the polarization dependence of the valence-band wave functions, the local spectra have been quantitatively analyzed in a manner which yields the energy and intensity dependence of the luminescence of strain-split hh and lh excitons. This approach allows for a determination of the spatial distribution of the stress tensor in GaAs/Si.

D.H.R. thanks Dr. B. G. Yacobi for useful discussions pertaining to the design of the optical-collection system used in this study. The research described in this paper was performed by the Center for Space Microelectronics Technology, Jet Propulsion Laboratory, California Institute of Technology, and was jointly sponsored by the Defense Advanced Research Projects Agency, and the National Aeronautics and Space Administration, Office of Aeronautics, Exploration, and Technology.

---

*Also at Geo-Centers, Inc., N. J. Operations, Lake Hopatcong, NJ 07849.

[1] S. Zemon *et al.*, Solid State Commun. **58**, 457 (1986); S. Zemon *et al.*, in *Gallium Arsenide and Related Compounds—1986,* Proceedings of the 13th International Symposium, edited by W. T. Lindley, IOP Conf. Proc. No. 83 (Institute of Physics and Physical Society, Bristol, 1987), p. 141.
[2] B. A. Wilson *et al.*, J. Electron. Mater. **17**, 115 (1988).
[3] Y. Huang *et al.*, Appl. Phys. Lett. **52**, 579 (1988).
[4] H. Shen *et al.*, J. Appl. Phys. **68**, 369 (1990).
[5] R. M. Lum *et al.*, J. Appl. Phys. **64**, 6727 (1988).
[6] T. D. Harris *et al.*, J. Appl. Phys. **64**, 5110 (1988).
[7] W. M. Duncan *et al.*, J. Appl. Phys. **59**, 2161 (1986).
[8] M. Enatsu *et al.*, Jpn. J. Appl. Phys. **26**, L1468 (1987).
[9] A. Freundlich *et al.*, Phys. Rev. B **40**, 1652 (1989).
[10] B. G. Yacobi *et al.*, Appl. Phys. Lett. **51**, 2236 (1987); B. G. Yacobi *et al.*, *ibid.* **52**, 555 (1988); B. G. Yacobi *et al.*, J. Cryst. Growth **95**, 240 (1989).
[11] T. Kanata *et al.*, Phys. Rev. B **41**, 2936 (1990).
[12] M. Dutta *et al.*, Appl. Phys. Lett. **57**, 1775 (1990).
[13] F. H. Pollak and M. Cardona, Phys. Rev. **172**, 816 (1968).
[14] M. Chandrasekhar and F. H. Pollak, Phys. Rev. B **15**, 2127 (1977).
[15] S. M. Vernon *et al.*, J. Cryst. Growth **77**, 530 (1986).
[16] H. C. Casey and R. H. Kaiser, J. Electrochem. Soc. **114**, 149 (1967).
[17] By examining the orbital-strain Hamiltonian matrix (see, e.g., Ref. 13) the following can be shown: (1) In the representation referred to ⟨001⟩, the lh and hh wave functions will not mix in the strain-split $j = \frac{3}{2}$ bands for $\sigma_\parallel = \sigma_\perp \neq 0$; (2) In the representation referred to ⟨110⟩ the lh and hh wave functions generally mix for $\sigma_\parallel > 0$ and $\sigma_\perp = 0$, but the mixing is negligibly small for GaAs; (3) In both ⟨110⟩ and ⟨001⟩ representations, lh and hh wave functions can measurably mix in the more general case when $\sigma_\parallel > \sigma_\perp > 0$.

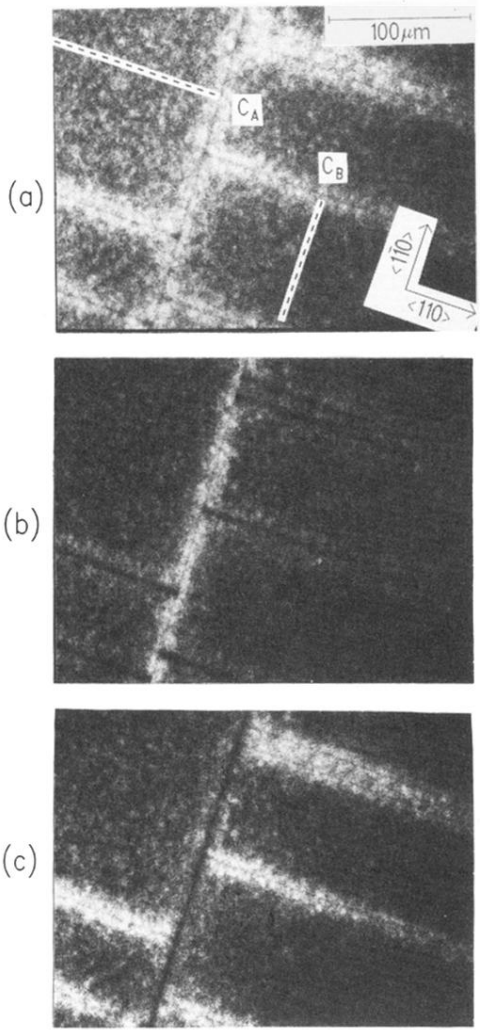

FIG. 1. Scanning monochromatic CL images at $h\nu = 1.494$ eV for the GaAs/Si sample with (a) no polarizer, (b) emission with $\mathbf{E} \parallel \langle 110 \rangle$, (c) and $\mathbf{E} \perp \langle 110 \rangle$. Two microcracks which run perpendicular and parallel to $\langle 110 \rangle$ are labeled C_A and C_B, respectively. The dashed lines indicate the positions of the electron beam during the localized spectroscopy measurements.